Dynamics of the anisotropy in decaying rotating turbulence with confinement effects

Cyprien Morize[1], Frédéric Moisy[1], Marc Rabaud[1] & Joël Sommeria[2]

[1]*CNRS, Univ Paris-Sud, Univ Pierre et Marie Curie-Paris6*
Lab FAST, Bat 502, Campus Univ, Orsay, F-91405, France
morize@fast.u-psud.fr

[2]*CNRS, Univ Grenoble 1 Joseph Fourier, INPG*
Lab LEGI/Coriolis, BP53, 38041 Grenoble cedex 9, France

Abstract :

The dynamics of the anisotropy of grid-generated decaying turbulence in a rotating frame is experimentally investigated by means of particle image velocimetry on the large-scale 'Coriolis' platform (LEGI, Grenoble). Turbulence is generated by rapidly towing a grid along a channel, providing a nearly homogeneous and isotropic initial state. Various integral scales are computed in order to characterize the growth of the anisotropy during the decay. As expected, the vertical correlation (aligned with the rotation axis) of the horizontal velocity is found to grow more rapidly than the others correlations. More surprisingly, a non trivial hierarchy between the remaining lengthscales is observed, as the consequence of Ekman pumping induced by the vertical confinement.

Résumé :

La croissance de l'anisotropie dans le déclin d'une turbulence de grille soumise à une rotation d'ensemble est étudiée expérimentalement par vélocimétrie par images de particules sur la plateforme 'Coriolis' (LEGI, Grenoble). La turbulence est générée pas la translation rapide d'une grille le long d'un canal, produisant un état initial approximativement homogène et isotrope. Différentes échelles intégrales sont calculées afin de caractériser l'anisotropie croissante de l'écoulement durant le déclin. Comme attendu, la corrélation verticale (le long de l'axe de rotation) de la vitesse horizontale croît plus rapidement que les autres corrélations. De façon plus surprenante, une hiérarchie entre les autres échelles intégrales est observée, et résulte du pompage d'Ekman induit par le confinement vertical de l'écoulement.

Key-words :

Turbulence ; Rotation ; PIV

1 Introduction

Turbulence subjected to system rotation is present in a wide range of applications, from engineering to geophysics and astrophysics. Although often coupled to other effects, such as stratification or confinement, rotating turbulence in itself is a delicate issue that is not completely understood. On the basis of the Taylor-Proudman theorem, rapidly rotating turbulence is often considered as being two-dimensional. However, the two-dimensionalization process itself, being driven by the nonlinear interactions, requires moderate Rossby numbers or asymptotically large times to take place, so strict two-dimensionality cannot provide a useful description of rotating turbulence. Moreover, in laboratory experiments, a much shorter time scale associated to the dissipation in the Ekman layers is present, leading to an even stronger limitation in a route towards this hypothetical two-dimensional state.

Rotation considerably affects the dynamics and the structure of turbulence through the Coriolis force, which causes inertial waves to propagate through the bulk of the fluid. The propa-

gation of these waves is anisotropic, and a preference for slow disturbances to propagate along the rotation axis is expected. The vertically elongated columnar structures observed in rotating turbulence are seen as a signature of this progressive anisotropization of the flow.

A useful characterization of the anisotropy and dimensionality of rotating turbulence is provided by the following set of integral length scales, defined from the correlation of the α velocity component along the β direction:

$$L_{\alpha\alpha,\beta} = \int_0^\infty C_{\alpha\alpha,\beta}(r)\, dr, \qquad C_{\alpha\alpha,\beta}(r) = \frac{\langle u_\alpha(\mathbf{x}) u_\alpha(\mathbf{x} + r\mathbf{e}_\beta)\rangle}{\langle u_\alpha^2\rangle}. \tag{1}$$

In decaying turbulence these lengthscales increase in time. While they all grow at the same rate for nonrotating isotropic turbulence, $L \sim t^{2/5}$, the anisotropy of rotating turbulence leads to different growth laws for the different lengthscales. The most remarkable feature is the decoupling between the longitudinal correlations of the longitudinal and transverse velocities along the rotation axis, $L_{11,3}$ and $L_{33,3}$, reported experimentally (Jacquin *et al.* (1990)) and numerically (Squires *et al.* (1994)). This decoupling originates from the Coriolis force, which affects only the velocity component perpendicular to the rotation axis (Canuto *et al.* (1997)). In the limit of vanishing Rossby numbers, phenomenological arguments suggest $L_{11,3} \sim t^{6/5}$ and $L_{33,3} \sim L_{\alpha\alpha,1} \sim t^{1/5}$ (Squires *et al.* (1994); Morize & Moisy (2006)).

In this paper, we present original measurements of the integral scales in decaying rotating turbulence by means of PIV (particle image velocimetry). In particular, we focus on the influence of the vertical confinement on the hierarchy of the various integral scales.

2 Experimental setup

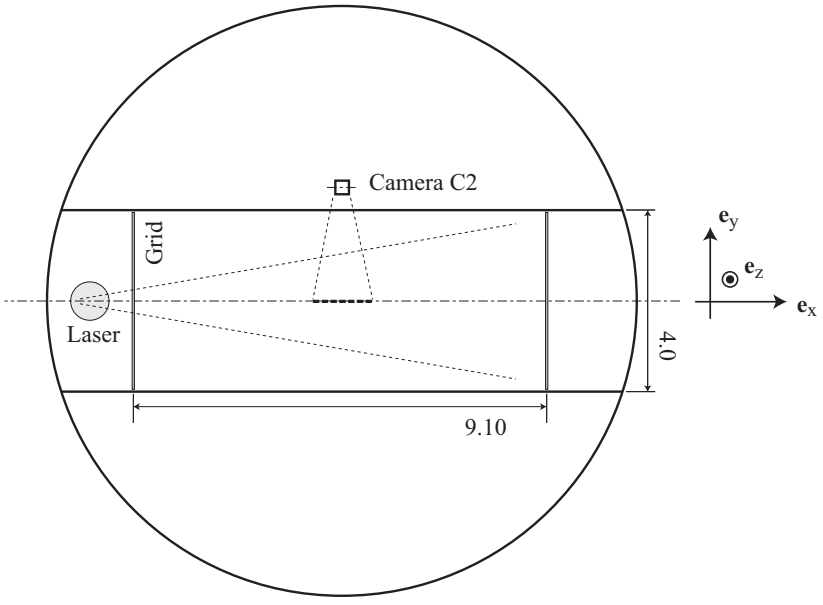

Figure 1: Experimental setup

The experimental setup, sketched in figure 1, consists in a 13 m $\times$4 m channel, mounted on the 'Coriolis' rotating plateform (see Praud *et al.* (2006) for details). The whole tank is filled with water with an average depth of 1 m. Turbulence is generated by towing a grid at a constant velocity $U = 30$ cm s^{-1} along the channel, over a distance of 9.1 m. The streamwise, spanwise

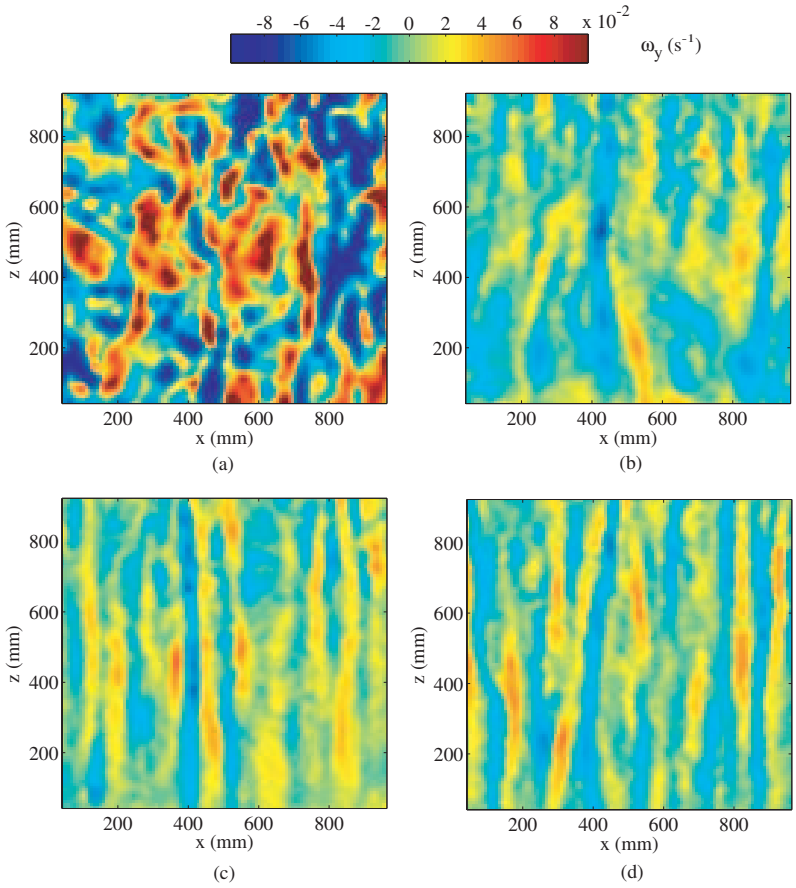

Figure 2: (Color) Horizontal vorticity fields ω_y obtained in a vertical plane, parallel to the rotation axis, at four successive times for $\Omega = 0.10$ rad s^{-1}. (a) $\tau = tU/M = 300$, (b) $\tau = 900$, (c) $\tau = 1400$ and (d) $\tau = 3500$. The imaged rectangle represents 1.1 m $\times$ 1 m.

and vertical axis are noted $\mathbf{e}_x$, $\mathbf{e}_y$ and $\mathbf{e}_z$ respectively. The grid is made of square bars of 36 mm, with a mesh size of $M = 17$ cm and a solidity ratio of 0.38. A high-resolution particle image velocimetry system, based on a 14 bits 2048×2048 pixels camera, was used in these experiments. The measurements were performed in a 1.1 m $\times$ 1 m area in the vertical plane $(\mathbf{e}_x, \mathbf{e}_z)$ in the middle of the channel ($y = 2$ m).

One experiment without rotation, and 3 experiments with rotation periods of 30, 60 and 120 s, have been carried out. The initial condition of an experiment is characterized by two nondimensional parameters, the Reynolds and Rossby numbers based on the grid velocity and the grid mesh,

$$Re_g = UM/\nu, \qquad Ro_g = U/2\Omega M.$$

The Reynolds number is kept constant for the four experiments, $Re_g \simeq 5 \times 10^4$. The Rossby number lies in the range 4.2-16.9, so that the turbulent energy production in the near wake of the grid is essentially unaffected by the rotation and the flow is initially tri-dimensional. As the instantaneous Rossby number, based on fluctuations velocity u', decreases during the energy decay, the relative influence of rotation progressively affects the entire flow. Since each realization of the decay is highly fluctuating, convergence of the statistics is achieved by computing ensemble averages for the same time delay t after the grid translation over 6 independent realizations of the decay.

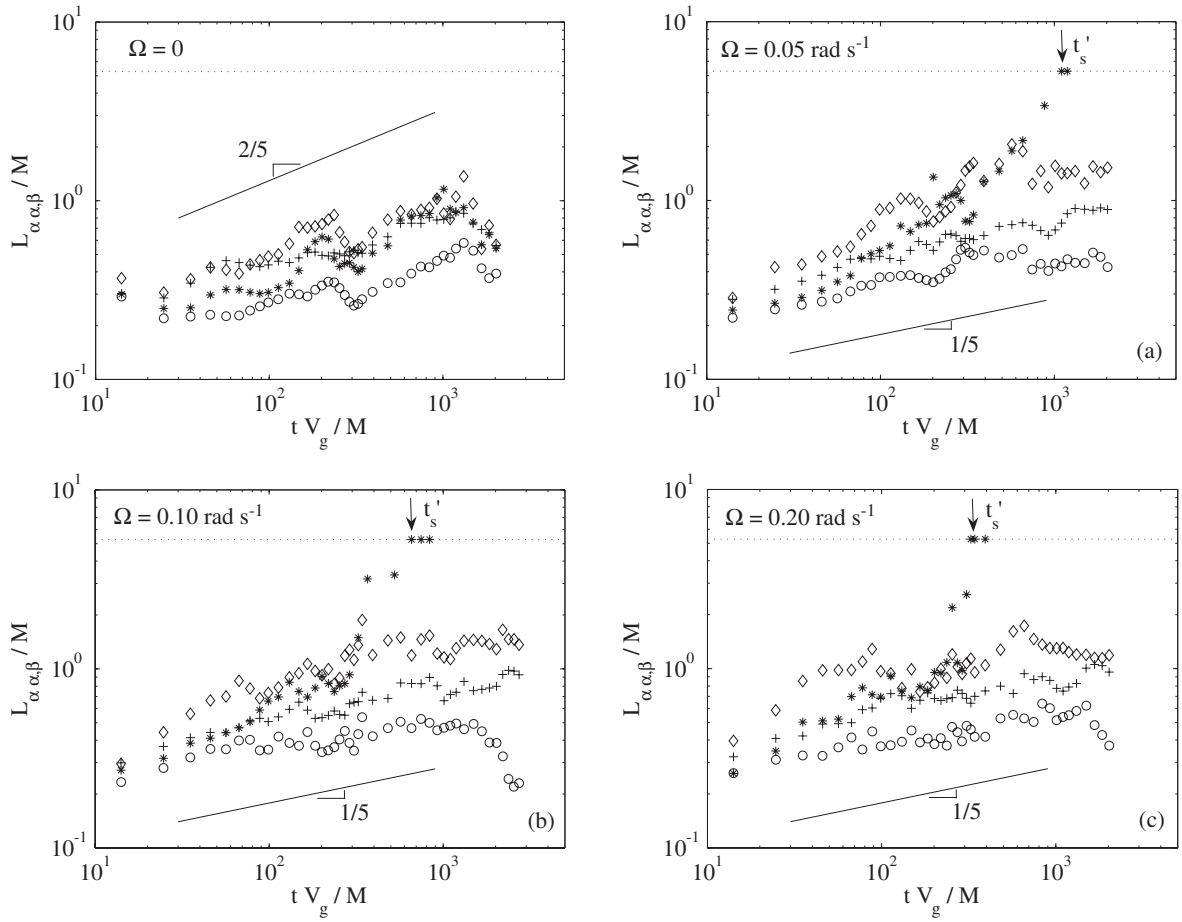

Figure 3: Normalized integral scales $L_{\alpha\alpha,\beta}/M$ as a function of time for: (a) $\Omega = 0.05$ rad.s^{-1}; (b) $\Omega = 0.05$ rad s^{-1}; (c) $\Omega = 0.10$ rad s^{-1}; (d) $\Omega = 0.20$ rad s^{-1}. The symbols $+$, $*$, $\circ$ and $\diamond$ correspond respectively to the integral scales $L_{11,1}$, $L_{11,3}$, $L_{33,1}$ and $L_{33,3}$. The full line shows a power law $t^{2/5}$, and the dashed lines shows $t^{1/5}$. The horizontal dotted lines correspond to the height of the tank normalized by the grid mesh, $h/M \simeq 5.9$. The arrows indicate the time of saturation of the integral scale to the height of the tank.

Figure 2 shows four snapshots of the horizontal component of the vorticity field, $\omega_y = \partial u_x/\partial z - \partial u_z/\partial x$, taken during the decay for $\Omega = 0.1$ rad s^{-1} and $U = 30$ cm s^{-1}. This quantity is essentially sensible to the shearing motion $\partial u_z/\partial x$ between vertical columnar structures.

Just after the grid translation, $\tau = tU/M \sim 300$ (Fig. 2(a)), the vorticity ω_y shows nearly isotropic small-scale disordered fluctuations. As time proceeds ($\tau \sim 900$ and 1400), nearly vertical columnar structures gradually appears, showing a strong vorticity (and hence velocity) correlation along the vertical direction.

3 Growth laws of the integral scales

From the velocity fields obtained in the vertical plane, 4 integral scales may be measured, defining the horizontal correlation of the u_x and u_z velocities, $L_{11,1}$ and $L_{33,1}$, and their vertical correlation functions, $L_{11,3}$ and $L_{33,3}$. However, both the finite depth of the channel and the insufficient statistics at large separations prevent from computing these integral scales directly from Eq. 1. Instead, we approximate $L_{\alpha\alpha,\beta}$ by truncating the integral of the correlation function

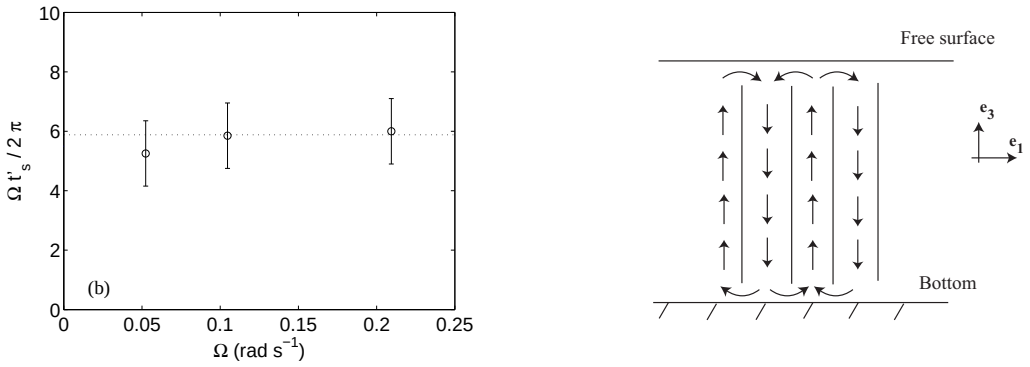

Figure 4: (a) Saturation time t'_s of the vertical scale normalized by the rotation period as a function of Ω. (b) Sketch of the vertical flow due to the Ekman pumping, responsible for the increase of $L_{33,3}$ and the decrease of $L_{11,3}$.

as

$$L_{\alpha\alpha,\beta} = \int_0^{r^*} C_{\alpha\alpha,\beta}(r)\, dr\ , \tag{2}$$

where r^* is the scale for which $C(r^*) = 0.2$. When $C(r)$ does not decrease below this threshold, $L_{\alpha\alpha,\beta}$ is taken equal to h by convention ($C_{\alpha\alpha,3}(r) = 1$ for all r for a strictly two-dimensional turbulence invariant along the vertical axis). Although this definition systematically underestimates the actual integral scales, the scaling measured from these quantities is expected to represent the actual evolution of the true lengthscales.

The time evolution of these 4 integral scales is shown in Figure 3. In the absence of rotation (fig. 3 (a)), a similar growth is obtained for all lengthscales. Although the scatter of the data prevents from a direct measurement of the exponent, we find that the growth laws are compatible with the power law $t^{2/5}$ expected for homogeneous and isotropic turbulence. In the presence of rotation (fig. 3 (b), (c) and (d)), the most striking effect is the rapid growth of $L_{11,3}$ (symbols $*$) compared to the 3 other ones. This rapid growth is a signature of a two-dimensionalisation of the flow, in good agreement with the experimental data of Jacquin *et al*. (1990) and the simulations of Squires *et al*. (1994). Above a saturation time t'_s, indicated by an arrow, the slow decrease of the correlation function does not allow to compute exactly $L_{11,3}$ from Eq. (2), which is taken equal to h by convention. As shown in figure 4 (a), this saturation time is found to verify

$$\frac{\Omega t'_s}{2\pi} \sim 5.5 \pm 0.5 \approx h/M, \tag{3}$$

i.e. $L_{11,3}$ roughly increases of one unit of mesh size M after each system rotation.

The scaling of the three other lengthscales, $L_{11,1}$, $L_{33,1}$ and $L_{33,3}$, is less evident from this figure. These three scales are expected to follow the same growth law, $L \sim t^{1/5}$ in the asymptotic regime. However, in our experiment, the vertical confinement probably plays an important role in the hierarchy of these three scales. Due to the zero velocity at the bottom wall, a vertical Ekman pumping takes place (see Fig. 4(b)). In the linear regime (low local Rossby number), this pumping induces a vertical velocity $|w_E| = (\nu\omega_z)^{1/2}$, ascending for anticyclonic vorticity ω_z and descending for cyclonic vorticity. In the nearly two-dimensional state, the horizontal flow consists in strong coherent vortices surrounded by shear layers. As a consequence, the coupling between the vertical components of the velocity and vorticity increases the vertical correlation $L_{33,3}$ (symbols $\Diamond$) and decreases the horizontal correlation of the vertical velocities,

$L_{33,1}$ (symbols $\circ$). The effects of the Ekman pumping may thus explain the observed ordering,

$$L_{33,1} < L_{11,1} < L_{33,3} \ll L_{11,3}.$$

This hierarchy is a distinctive feature of decaying rotating turbulence with confinement, and is in contrast with the numerical simulations in infinite medium or periodic boundary conditions, where no distinction between the first first 3 lengthscales is observed.

4 Conclusion

To summarize, a clear evidence of the growing anisotropy of the flow by the background rotation has been observed during the energy decay. In agreement with previous study, the vertical correlation of the transverse velocity, measured by the integral scale $L_{11,3}$, is found to increases more rapidly than the other correlations. In particular, the growth of $L_{11,3}$ is found to be compatible with law in $t^{6/5}$ proposed in the asymptotic regime. More interestingly, the 3 remaining integral scales show a nontrivial hierarchy, as the result of the Ekman pumping induced by the vertical confinement. These results highlight the complex interplay between the intrinsic growing anisotropy of decaying rotating turbulence, and the additional anisotropy induced by the boundary conditions.

References

Canuto, V.M., Dubovikov, M.S., 1997, A dynamical model for turbulence. V. The effect of rotation. *Phys. Fluids*, pp. 2132-2140, **9** (7).

Jacquin, L., Leuchter, O., Cambon, C., Mathieu, J., 1990, Homogeneous turbulence in the presence of rotation. *J. Fluid Mech.*, pp. 1-52, **220**.

Morize, C., Moisy, F., 2006, Energy decay of rotating turbulence with confinement effects. *Phys. Fluids*, pp. 065107, **18** (6).

Pedlosky, J., 1987, Geophysical fluid dynamics. *Springer-Verlag*.

Praud, 0., Sommeria, J., Fincham, A., 2006, Decaying grid turbulence in a rotating stratified fluid. *J. Fluid Mech.*, pp. 389-412, **547**.

Squires, K.D., Chasnov, J.R., Mansour, N.M., Cambon, C., 1994, The asymptotic state of rotating homogeneous turbulence at high Reynolds number. *74th Fluid Dynamics Symposium on "Application of Direct and Large Eddy Simulation to Transition and Turbulence"*, Chania, Greece, 4-1.